12-2021

Helicopter Flight Energy Modeling and Scaling for Urban Air Mobility Applications

Nolan Gene Hopkins

Helicopter Flight Energy Modeling and Scaling for Urban Air Mobility Applications

by

Nolan Gene Hopkins

A thesis submitted to the College of Engineering and Science of
Florida Institute of Technology
in partial fulfillment of the requirements
for the degree of

Master of Science
in
Aerospace Engineering

Melbourne, Florida
December, 2021

We the undersigned committee hereby approve the attached thesis,
"Helicopter Flight Energy Modeling and Scaling for Urban Air Mobility Applications."
by
Nolan Gene Hopkins

_____

Brian Kish, Ph.D.
Associate Professor
Aerospace, Physics and Space Sciences
Major Advisor

_____

Markus Wilde, Ph.D.
Associate Professor
Aerospace, Physics and Space Sciences

_____

Isaac Silver, Ph.D
Graduate Faculty
College of Aeronautics

_____

David Fleming, Ph.D.
Associate Professor and Department Head
Aerospace, Physics and Space Sciences

Abstract

Title: Helicopter Flight Energy Modeling and Scaling for Urban Air Mobility Applications

Author: Nolan Gene Hopkins

Advisor: Brian Kish, Ph.D.

The costs associated with conducting full-scale helicopter flight tests in terms of both time and money beg to question the validity of using small-scale model helicopters in order to predict full-scale performance. To do this, the energy change for a small time interval is determined throughout a full-scale helicopter's flight of a given profile, and the overall energy use compared to model results. The profile is then scaled based on a variety of factors, and the accuracy of energy scaling compared for each. Scaling dimensions based off helicopter weight and energy reserve modeling show promising results, but comparison of relative energy usage does not, and reasonings for these conclusions are shared.

Table of Contents

List of Figures

List of Tables

Acknowledgement

This project would not be possible without the support from the Federal Aviation Administration. Their funding and industry expertise has been pivotal in the research initiative for Urban Air Mobility at Florida Tech. They have coordinated conference calls with industry specialists for the benefit of this research.

Additionally, I would like to thank Danny Melnik and Manny Rodriguez of AeroPanda LLC for their assistance with completing the subscale testing. Without their help, this would not have been possible to do.

Dedication

I would like to dedicate this paper to my parents. They have supported me throughout my academic career and have pushed me to finish both my undergraduate and graduate degrees. I would not be where I am currently without their motivation, patience, and support.

Chapter 1
Introduction

The concept of urban air mobility is a fairly recent one, though the idea for rapid aerial transit around cities itself is not a novel one. One need only recall the "helicopter airlines" of the late 1950's and 1960's for proof that the idea of short, point-to-point flights via rotorcraft around metropolitan centers have been considered for many years. To that end, a study was done by Dajani, Stortstrom, and Warner[1] in early 1977 to examine the economic feasibility of helicopter passenger service, since many of the aforementioned airlines had run into financial troubles after a $50 million subsidy ran out in 1965. They found that helicopters could be useful for providing alternative airport access and impetus for VTOL intercity flights, but also noted that the demand for such a service was not properly developed at the time. Today, the prevalence of unmanned aerial drones and their use has given the average consumer more exposure to the idea of "air taxis", as well as development of the technology behind them, means that the concept of urban air mobility may yet now be a feasible one.

However, though the technology has matured, there are still issues that need to be resolved for this to work. First, the question of autonomous flight versus piloted flight is not one to be taken lightly, as in the case of an emergency, the benefit to having a trained pilot could save many lives. Second, many cities that may serve as ideal markets for this service do not yet possess the specialized infrastructure needed to accommodate it. Most importantly, though, is the development of reliable, lightweight battery technology. Many prospective UAM groups imagine using electric power as their primary energy source, much the same as small drones use but on a larger scale. The problem with that assumption is the amount of payload carried; small drones need not carry significant weight as a part of their regular operation, whereas UAM craft not only carry significant

[1] (Dajani, Stortstrom, and Warner, *Potential for Helicopter Passenger Service* 1977)

payload, but passengers whose safety must be assured as much as possible. As there are still shortcomings to be addressed with the technology, it is sensible to examine traditional combustion engines as a possible powerplant.

To study combustion-based VTOL flight, the most readily available aircraft are helicopters. With significant presence in the tourism and emergency services market, a similar subscale in nitromethane RC helicopters possible, and being capable of flying a simulated UAM flight profile, they are a logical substitute to test the feasibility of energy scaling laws for the UAM space. An additional benefit that could arise from determining a method to scale energy usage is that subscale testing is often far cheaper and quicker to do, such that if a scaling method proves sufficiently reliable, it is proposed that subscale testing could be used for a portion of the flight testing for new rotorcraft to save both time and money.

Chapter 2
Sample Flight Profile

A logical first step before testing any model is to define a sample flight profile to test. The flight profile for this case arises from the need to flight test aircraft intended for use in urban air mobility missions which by design are short, point-to-point flights. This requires a vertical takeoff (1), 6º climb to 2000 feet AGL (2), cruise phase (3), descent to an intermediary altitude of 500 feet AGL (4), a 60 second holding pattern above the landing site (5), and a final approach (6) and vertical landing at the site (7). 10 nautical miles is used as the distance from the takeoff site to the landing site, in order to mimic the UAM mission of ferrying passengers from a downtown area to the city's international airport. The sample flight profile is presented below in Figure 1 and Table 1; note that a starting altitude of 50 feet MSL is used due to the conditions at the test site. Figure 2 presents a reference ascent/descent profile, which will also be tested to further examine the impact of the cruise phase on energy use.

Table 1: Sample Flight Profile Segments

Segment Number	**1**	**2**	**3**	**4**	**5**	**6**	**7**
Initial Alt. (MSL) ft	50	70	2050	2050	550	550	70
Final Alt (MSL) ft	70	2050	2050	550	550	70	50
Time (sec)	10	t_{climb}	t_{cruise}	$t_{descent}$	60		15
Distance (nmi)		d_{climb}	$10 - d_{climb} - d_{descent}$	$d_{descent}$			
Gradient		6°		-9°			

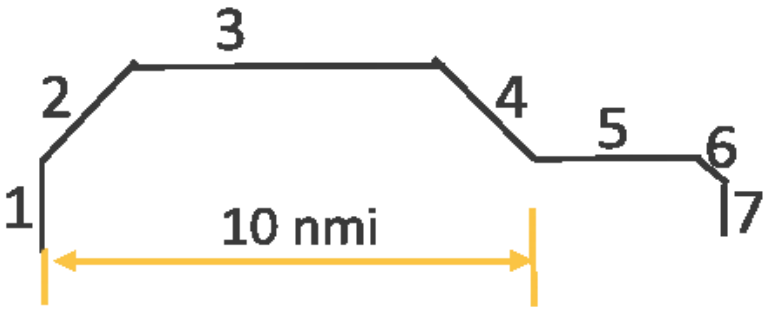

Figure 1: Sample UAM Flight Profile

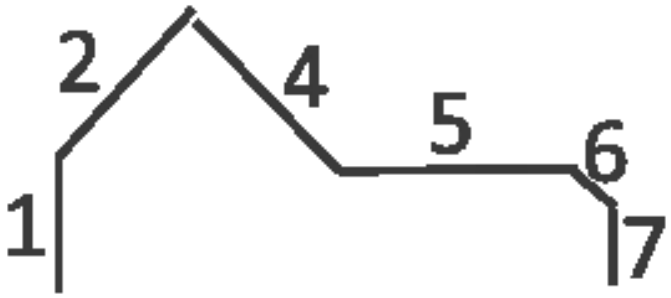

Figure 2: Ascent/Descent Flight Profile

Chapter 3
Modeling the Energy State and Proposed Scaling Laws

In order to model the energy state of a helicopter at any given point in flight, it is necessary to decide upon a method of approach from which to attack the problem. Several methods were tested of increasing complexity, as if the simplest model will approximate energy requirements with sufficient accuracy, then a more complex one will only offer diminishing returns to accuracy as a trade-off for increased on-board resource requirements should the method be used aboard.

Basic Energy State

The most basic energy state of a helicopter is that it converts the chemical energy in its fuel to changes in gravitational potential energy and kinetic energy, with losses in energy due to heat, drag on the helicopter, and other associated factors. To that end, the change in energy state of a helicopter over a discrete interval is given by the following:

$$E_t = F(E_{t-1} + m_{t-1}g(h_t - h_{t-1}) + \frac{1}{2}m_{t-1}(v_t^2 - v_{t-1}^2))$$

(1)

It is important to note that the helicopter mass changes throughout flight as fuel is burned, which necessitates a function to calculate the change in mass between time steps; this can be iterated once the new energy state is known as seen below:

$$m_t = m_{t-1} - (E_t - E_{t-1})Q$$

(2)

Though this method is certainly simple and easy to implement, it is too simplistic in its consideration of all factors that can affect the overall energy use of a helicopter. For instance, the propulsive efficiency is not considered at all, and different flight regimes

require different amounts of energy (i.e. it requires less energy to cruise than vertical flight). As such, this model was discarded in favor of the following.

Power Required Energy State

The power required for a helicopter's flight at any point can be calculated using methods proposed by Raymer[2] for three different flight regimes: vertical climb or hover, level forward flight, and climbing forward flight. These are likened to the vertical takeoff, climbing or descending, and cruise phases of a sample flight profile to be proposed in Section IV. For the first phase of flight, momentum theory is used to determine the induced inward velocity of air flowing through the rotor disk in terms of thrust disk loading. From there, the actual power required is derived using measure of merit and an estimation of total power produced by the helicopter between the main and tail rotors; this, combined with consideration of the extra requirements for climbing and ground effect) leads to the following equation:

$$P_{takeoff} = \left(\frac{fW}{M} \sqrt{\frac{f\left(\frac{W}{S}\right)}{2\rho}} + \frac{W v_{climb}}{2} \right) \left(\frac{1 + \left(\frac{P_{tail}}{P_{main}}\right)}{\eta_{mech}} \right) \quad (3)$$

[2] (Raymer, *Aircraft Design: A Conceptual Approach* 2012)

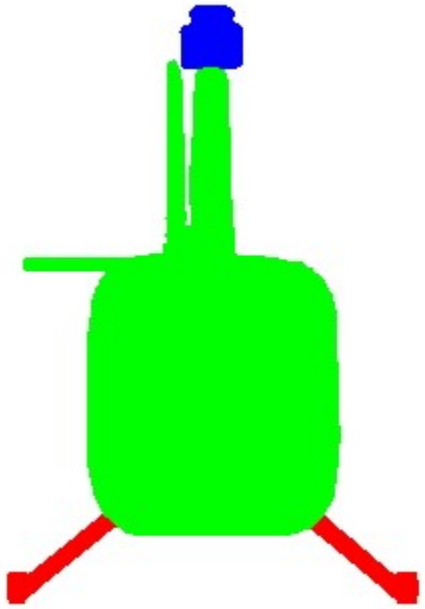

Figure 3: R44 Frontal Area Profile

For the climbing, descending, and cruise phases, the rotor is treated as both a wing and propeller of a traditional airplane, with empirical data used to assume various constants. Oswald's efficiency factor is used to estimate induced drag of the helicopter, whereas parasitic drag is determined using the drag area of the frontal profile of the helicopter. The drag area is determined via percentage of frontal area occupied by various components, as seen in Table 2.

Table 2: Parasitic Drag Area Ratios

Component	D/q per unit frontal area
Fuselage	0.07-0.1
Landing Skid	1.01
Rotor Hub	1.0-1.4

These values are used in the Equation (4) to determine the total drag area.

$$\left(q\left(\frac{D}{q}\right)\right)_{total} = \sum q_{component}(D/q)_{component} \tag{4}$$

For a Robinsion R44, the total drag area is determined with Figure 1 taken from the pilot's handbook[3], with green indicating a fuselage component, blue the rotor hub, and red for landing skids. A scaling factor of 299 pixels to 129 inches was measured, and the respective frontal areas calculated in Table 3.

Table 3: R44 Frontal Area

Component	Frontal Area (in^2)
Fuselage	19747
Landing Skid	1282
Rotor Hub	882

With this information determined, the following formula is used to compute the power required for forward flight:

$$P_{climbing} = \frac{v}{\eta_p}\left[\left(q\left(\frac{D}{q}\right)\right)_{total} + \frac{W^2}{4eqS} + W sin\gamma\right]\left(\frac{1+\left(\frac{P_{tail}}{P_{main}}\right)}{\eta_{mech}}\right) \tag{5}$$

Note that for this formula to be used for cruise, the flight path angle is assumed to be a small angle ($\gamma \leq 5^o$) and the associated term is assumed to be zero. This is seen in Equation 6, the power required for cruise:

[3] (Robinson, *R44 Pilot's Operating Handbook* 2007)

$$P_{cruise} = \frac{v}{\eta_p}\left[\left(q\left(\frac{D}{q}\right)\right)_{total} + \frac{W^2}{4eqS}\right]\left(\frac{1+\left(\frac{P_{tail}}{P_{main}}\right)}{\eta_{mech}}\right) \quad (6)$$

Though the determination of which flight phase is currently ongoing is simple for climbing and cruise, a separate threshold is used to determine vertical climb based on rotor diameter. If the helicopter is within one rotor diameter of the ground, it is assumed to be in ground effect and Equation 3 is used, whereas if the helicopter is more than one rotor diameter away from the ground, Equations 5 and 6 are used. If the flight path angle is greater than 5 degrees, the helicopter is assumed to be climbing or descending, thus requiring Equation 5. Otherwise, if the flight path angle is small, the helicopter is cruising, and for that Equation 6 is used. The power required is then multiplied by the time step to determine energy usage for said interval.

Scaling Factors

The justification of choosing scaling factors depends upon which aspect is seen as most important to preserve between large and small-scale flights. Several key parameters of helicopter dynamics come to mind, but the three most important are rotor diameter, maximum disk loading, and maximum advance ratio. A ratio of rotor diameters is the simplest to calculate, as the data needed is provided by a pilot's handbook or from direct measurement. As this is akin to using wingspan as a scaling factor for conventional aircraft, the methodology could therefore prove viable for helicopters as well. Maximum disk loading, therefore, translates to the maximum wing-loading of conventional aircraft, and considers aircraft weight, which may vary significantly between small- and full-scale helicopters due to powerplant size. The equation for this ratio is given below in terms of maximum takeoff weight (W_{MTO}):

$$R_{W/S} = \frac{\left(\frac{W_{MTO}}{S}\right)_{subscale}}{\left(\frac{W_{MTO}}{S}\right)_{fullscale}}$$

(7)

A third scaling factor proposed is the use of advance ratio. This characteristic is one of the six kep similarity parameters proposed by Hunt[4] in the analysis of similarity requirements for helicopter rotors as it relates the relative motion of undisturbed air and the helicopter rotor. As such, the following ratio based on advance ratio is proposed to be as follows:

$$R_J = \frac{(J_{max})_{subscale}}{(J_{max})_{fullscale}} = \frac{\left(\frac{v_{max}}{\Omega_{max} d}\right)_{subscale}}{\left(\frac{v_{max}}{\Omega_{max} d}\right)_{fullscale}}$$

(7)

Furthermore, a fourth scaling concept derives from the method proposed by Chambers[5] as intended for fixed-wing aircraft scaling. This method consists of using the ratio of the aircraft's primary geometric parameter (i.e. wingspan) and applying it to other characteristics with an exponent applied, as seen below.

Table 4: Chambers Scaling Law and Proposed Helicopter Equivalencies

Aircraft Property	Helicopter Equivalency	Scaling Factor
Wingspan	Rotor Diameter	N
Length	Length	N
Wing Area	Rotor Area	N^2
Aspect Ratio	Rotor Aspect Ratio	1
Chord Length	Rotor Chord	N
Empty Weight	Empty Weight	N^3
Max Takeoff Weight	Max Takeoff Weight	N^3
Max Power	Max Power	$N^{3.5}$
Total Fuel Capacity	Total Fuel Capacity	N^3
Reynolds Number	Reynolds Number	$N^{1.5}$

[4] (Hunt, *Similarity Requirements for Aeroelastic Models* 1972)
[5] (Chambers, *Modeling Flight* 2010)

A tabulation of the proposed scaling laws are provided in Table 5 below.

Table 5: Scaling Law Summary

Scaling Law	Calculated Ratio
Rotor Diameter	0.1342
Maximum Disk Loading	0.1733
Maximum Advance Ratio	0.1926
Chambers Method	See Tables 4 and 6

An alternative method of using Chambers' scaling law is to instead scale based on a different parameter and use dimensional analysis to adjust the other parameters appropriately; this method is summarized in Table 6 with maximum power as the scaling factor.

Table 6: Alternative Chambers Scaling Law Based on Max Power

Aircraft Property	Helicopter Equivalency	Scaling Factor
Wingspan	Rotor Diameter	$N^{1/3.5}$
Length	Length	$N^{1/3.5}$
Wing Area	Rotor Area	$N^{2/3.5}$
Aspect Ratio	Rotor Aspect Ratio	1
Chord Length	Rotor Chord	$N^{1/3.5}$
Empty Weight	Empty Weight	$N^{3/3.5}$
Max Takeoff Weight	Max Takeoff Weight	$N^{3/3.5}$
Max Power	Max Power	N
Total Fuel Capacity	Total Fuel Capacity	$N^{3/3.5}$
Reynolds Number	Reynolds Number	$N^{1.5/3.5}$

Chapter 4
Test Method and Results

To test the effectiveness of the model against real-world results, the sample profiles in Section III are flown in a Robinson R44, with a GoPro attached inside the cockpit for data collection. A picture of the helicopter used is given in Figure 4, with the test team standing in front of it. Three tests of each profile were flown to ensure ample data was collected for each profile, for a total of six flights. The R44 flights were conducted at Kissimmee, FL, whereas the scale model, an Align TREX 600N chosen for its availability and combustion-based powerplant, was flown at a field in Palm Bay, FL known locally as The Compound. A picture of this test asset in its packed configuration is given in Figure 5, with the main rotor blades stowed for transport to the test site.

Figure 4: Test Helicopter with Test Team in Front

Figure 5: Test Subscale Helicopter in Packed Configuration

R44 Test Flights

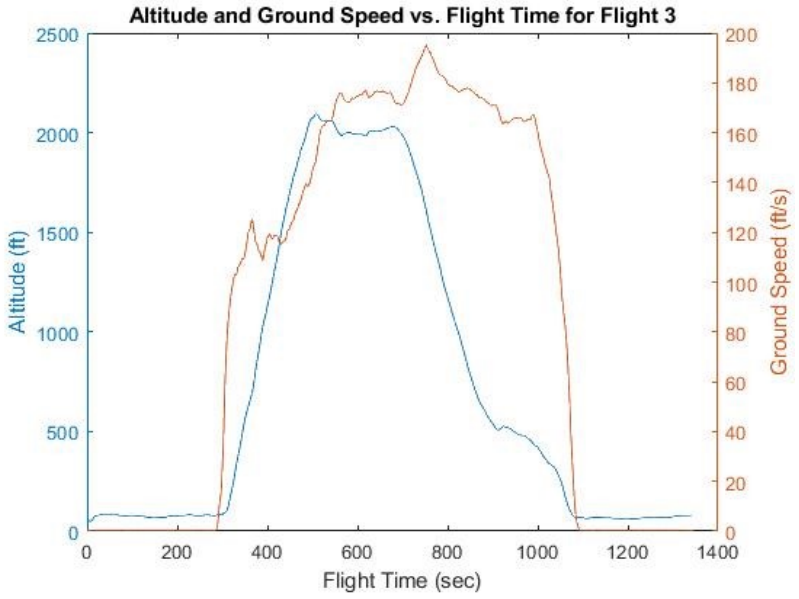

Figure 6: UAM Profile Altitude/Speed vs. Flight Time

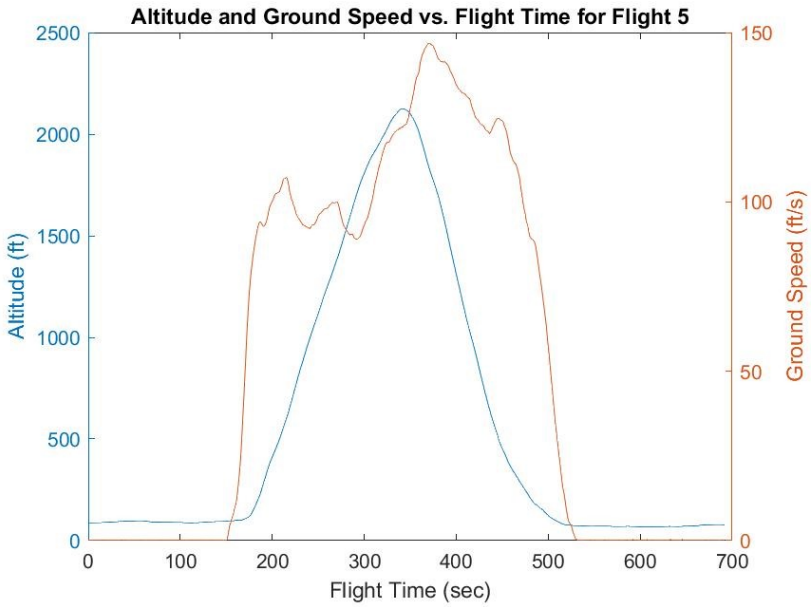

Figure 7: Ascent/Descent Profile Altitude/Speed vs. Flight Time

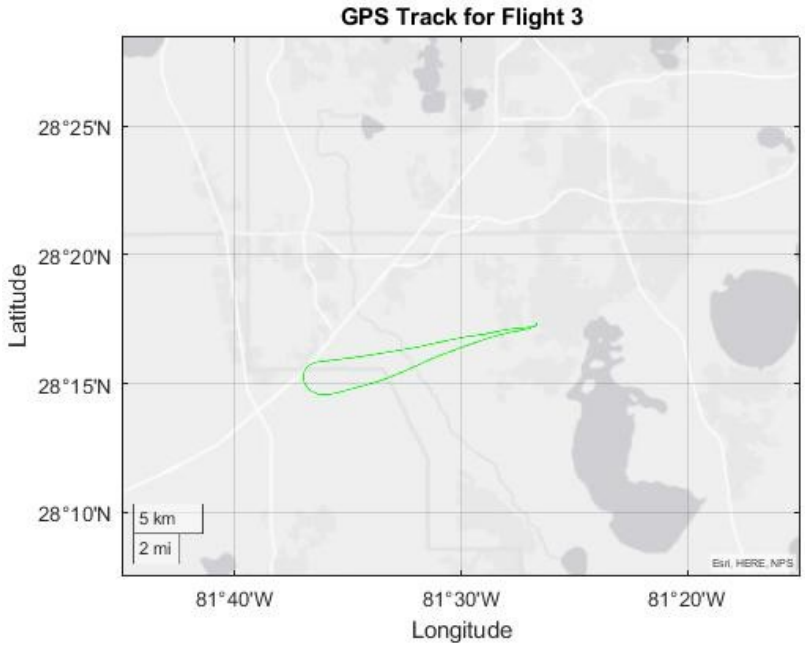

Figure 8: UAM Test Profile GPS Track

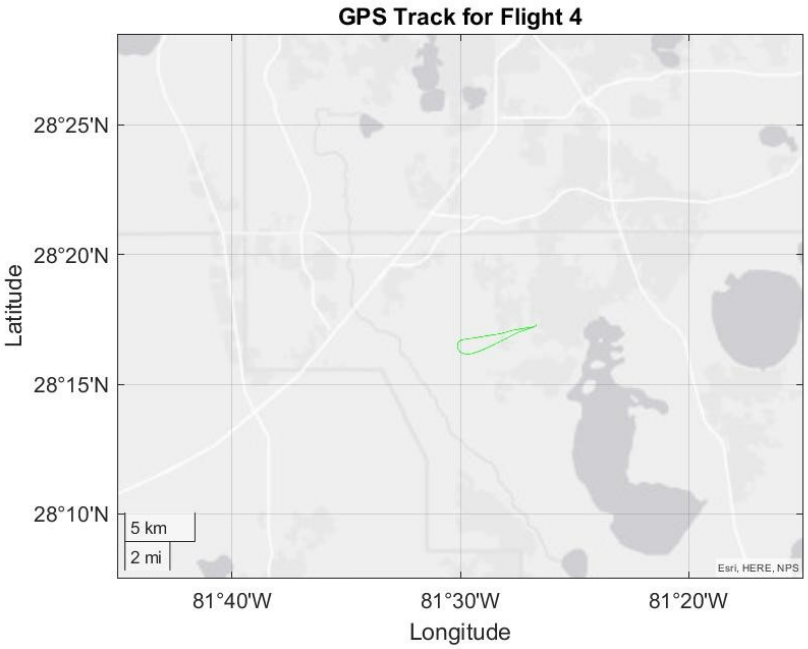

Figure 9: Ascent/Descent Profile GPS Track

To obtain flight data from the R44, a GoPro camera was mounted inside the cockpit. GPS data from the GoPro provides not only altitude and GPS coordinates, but also groundspeed. An altitude/speed plot and GPS track for the are provided below in Figures 6 through 9. Flight 3 was used as a sample for the test profile and Flight 5 was used for the ascent/descent profile. Data on fuel flow was obtained from the fuel required to refill the helicopter's tanks and is presented in Table 7. Note that Flight 6 is omitted from the data; this is due to the fact that the test itself was interrupted by air traffic in the area, and as such, the results from it are not usable for this work.

Table 7: R44 Fuel Use

Flight Number	Profile Type	Total Fuel Use (gal)
1	UAM Test	4.0
2	UAM Test	4.2
3	UAM Test	3.4
4	Ascent/Descent	2.0
5	Ascent/Descent	1.9

TREX 600N Test Flights

To conduct the small-scale test flights, a track was laid out at the test area using the intersections of roads as the endpoints. To accurately determine when the helicopter reaches each endpoint, a spotter stands at each point and alerts the pilot when the helicopter reaches the end of the track. An overhead diagram of the test area is presented in Figure 10, with the track outlined in red, spotter locations in purple, flight line in yellow, and flight line denoted.

Using a scaling factor of 63 pixels per 100 feet, as determined by the scale in the bottom-right corner of the figure, the track is determined to be 698 feet long. For the purpose of analysis, it is assumed that the helicopter flew in straight lines, as the pilot would sometimes marginally overshoot the turn and other times would turn a small distance before the turn. Using this track, six flights were conducted. The first three flights

Figure 10: 600N Test Area Overhead Map

consisted of an immediete takeoff, climb to a cruising altitude of 40 ft, and cruise for a set number of laps around the track. As this does not complete the entire UAM test profile, due to piloting difficulties, it is treated as the cruise portion of the UAM profile; from this point on, it is referred to as the cruise profile. The tabulation of the data from these flights is presented in Table 8. The latter trio of flights consisted of a single full lap around the track, with the first half of the lap a constant climb from the ground to 40 ft and the latter a constant descent back to the starting point. The data from these flights is presented in Table 9. Note that percent error refers to dividing the deviaiton by the average.

Table 8: Cruise Profile Test Data

Flight Number	Lap Count	Flight Distance (ft)	Flight Time	Average Lap Time (sec)	Average Airspeed (ft/sec)	Fuel Used (mL)	Average Fuel Flow (mL/sec)
1	5	6980	2:53.43	34.69	40.25	130	0.7496
2	8	11168	3:44.03	28.00	49.85	220	0.9820
3	10	13960	4:59.32	29.93	46.64	230	0.7684
Average				30.87	45.58		0.8333
Deviation				3.443	4.887		0.1291
Percent Error				11.15	10.72		15.49

Table 9: Climb/Descent Profile Test Data

Flight Number	Lap Count	Flight Distance (ft)	Flight Time	Average Lap Time (sec)	Average Airspeed (ft/sec)	Fuel Used (mL)	Average Fuel Flow (mL/sec)
4	1	1396	01:09.0	69.00	20.23	30	0.4348
5	2	2792	01:32.7	46.35	30.12	70	0.7551
6	1	1396	58.73	58.73	23.77	30	0.5108
Average				58.03	24.71		0.62
Deviation				11.34	5.01		0.17
Percent Error				19.55	20.28		29.52

Energy Use Comparison

The total energy used to fly each profile is found in Table 10. The energy usage is presented as a percentage of initial energy capacity as determined by fuel tank capacity and energy content of the fuel. For the R44, a nominal tank capacity of 29.5 gallons is used, whereas the TREX 600N has a fuel tank with a capacity of 440 mL, or 0.1162 gallons. The energy density of 100LL Avgas, as used by the R44, is 112182 BTUs per gallon[6]. The fuel used by the TREX 600N is a mix that contains 30% nitromethane, 47% methanol, and 23% lubricants that are not combusted[7]; the energy density of the nitromethane mixture is calculated by using established values for each component's energy content[8][9], in MJ/kg, and the respective density to determine an energy content in BTUs per gallon. These values come to 30120.38 BTU/gal for pure nitromethane and 28346.53 BTU/gal for pure methanol. To determine the total energy capacity, the mixture percentages are multiplied by the energy density of each component and added together before being multiplied by the fuel capacity of the helicopter. This value is represented in Table 10 as the Initial Energy Capacity.

Table 10: Energy Usage Comparison

Aircraft	Initial Energy Capacity (BTUs)	UAM Test Profile Usage (% of Initial)	Cruise Profile Usage (% of Initial)	Ascent/Descent Profile Usage (% of Initial)
R44	3318750	13.56	N/A	8.70
TREX 600N	2598.11	N/A	52.27	18.18

Additionally, energy state plots are provided below in Figures 12 and 13 for one of each of the full-scale flights.

[6] (Warter Aviation, *100LL Avgas*)
[7] (Lewis, *Morgan Fuels Product Analysis* 2020)
[8] (LUMITOS, *Nitromethane*)
[9] (Hua, *Energy Density of Methanol* 2005)

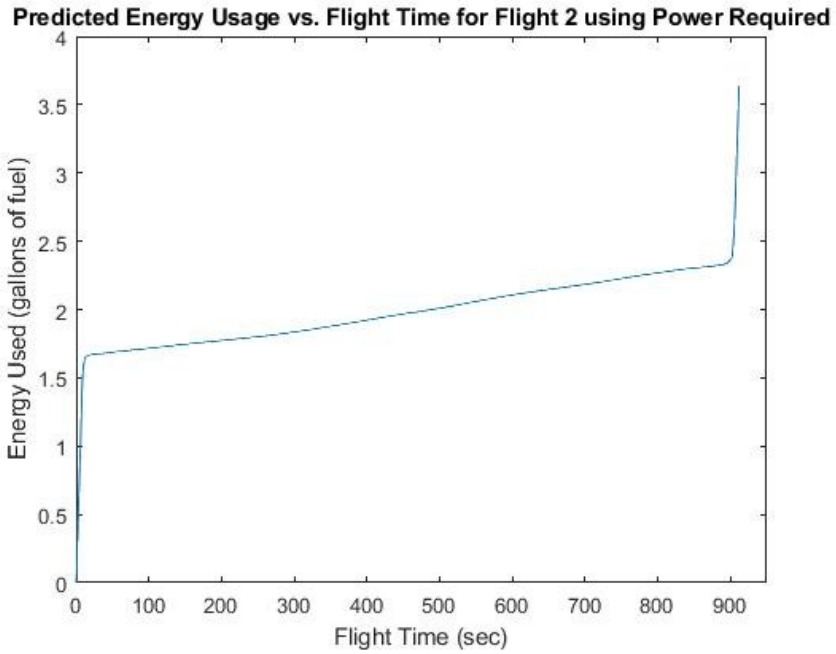

Figure 11: UAM Test Profile Modeled Energy Reserves

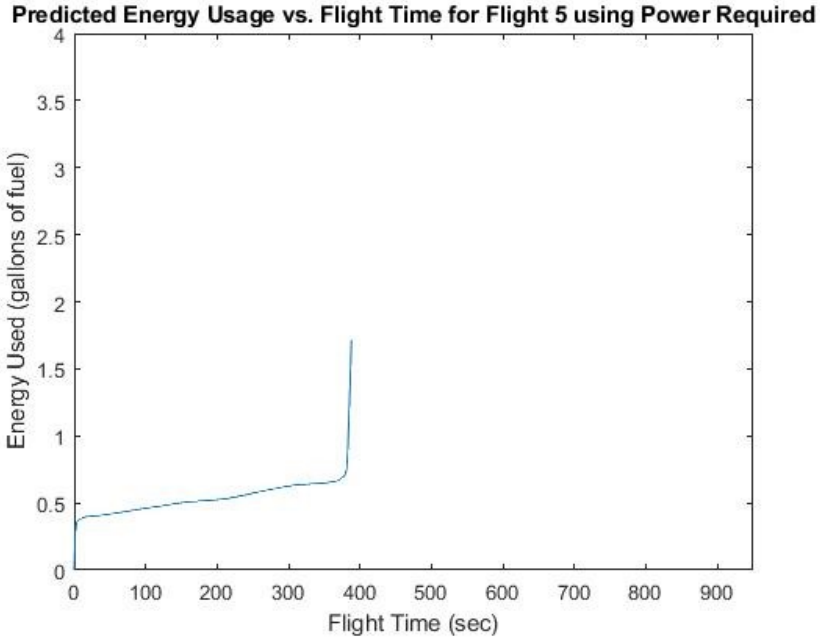

Figure 12: Ascent/Descent Profile Modeled Energy Reserves

Comparisons of the model results to the R44 data are found below in Table 11. The energy usage predicted by the model for the course of the flight is determined via cross-referencing the times of takeoff and landing from the GoPro mentioned previously. An attempt to gather real-time fuel use data was made as well, but the R44 fuel gauges possessed insufficient accuracy to get any useful data from it. Both the main and auxiliary tank gauges were expressed as percentages of a full tank, and this would not suffice to compare with real-time data accurately.

Table 11: Power Required Model Fuel Usage Comparison

Flight Number	Model Fuel Usage (gal)	Actual Fuel Usage (gal)	Model Percent Error
1	3.91	4	2.25
2	3.65	4.2	13.10
3	3.73	3.4	9.71
4	1.88	2.0	6.00
5	1.72	1.9	9.47

Chapter 5
Analysis

To examine the scaling law validity, a sample scaled helicopter is designed based off the R44 using the various proposed scaling laws. Of the dimensions proposed the most accurate method found was the Chambers method using weight as the scaling parameter; this is shown in Table 12 below. On a parameter-by-parameter average, using weight as the scaling parameter of choice creates a sample scale helicopter most similar to the 600N. The results of using other proposed scaling factors to create a sample scaled helicopter are presented in Table 13.

Table 12: Chambers Scaling Law Comparison

Dimension	R44	600N	Rotor Diam.	Max Power	Rotor Area	Weight	Re
Rotor Diam.(ft)	33	4.43	4.43	8.68	4.43	5.21	3.23
Length (ft)	30	3.81	4.03	7.89	4.03	4.74	2.94
Rotor Area (ft^2)	855.30	15.41	15.41	224.97	15.41	21.33	8.19
AR	1.27	1.27	1.27	1.27	1.27	1.27	1.27
Chord (ft)	0.86	0.18	0.12	0	0.12	0.14	0.08
Empty Weight (lbs)	1450	7.05	3.51	26.39	3.51	5.71	1.36
Max Weight	2500	7.81	6.05	45.5	6.05	9.85	2.34
Max Power (hp)	225	2.1	0.2	2.1	0.2	0.35	0.07
Fuel Capacity (gal)	29.5	0.1162	0.07	0	0.07	0.12	0.03
R_e	45890176	1405263	2257118	11822	2257118	2880127	1405263

Table 13: Simple Scaling Law Comparison

Dimension	R44	600N	Rotor Diameter	Max Disk Loading	Max Advance Ratio
Rotor Diam. (ft)	33	4.43	4.43	5.72	6.36
Length	30	3.806	4.03	5.20	5.78
Rotor Area (ft^2)	855.30	15.42	114.78	148.22	164.73
Rotor AR	1.27324	1.27	0.17	0.22	0.25
Chord (ft)	0.86	0.18	0.12	0.15	0.17
Empty weight (lbs)	1450	7.05	194.59	251.29	279.27
Max Weight	2500	7.81	335.50	433.25	481.50
Max Power (hp)	225	2.1	30.20	38.99	43.34
Fuel Capacity (gal)	29.5	0.12	3.96	5.11	5.68
R_e	45890176	1405263	6158461	7952767	8838447

Looking at the average percent error across each methodology is minimized when using weight as the scaling parameter; this value is 8.45 percent. Considering that the R44 and 600N were not specifically designed with scaling in mind, this error is more than acceptable. From the modeling aspect, there is relatively much less error as compared to the energy usage results. All errors are within 15 percent, which, given the nature of the testing method used, is acceptable. The most interesting results, however, are found in the energy usage and test flight data.

Initial impressions from the test flights are that the data from the subscale testing contains other interesting trends. Firstly, there is drastically increased fuel usage as a percentage of initial capacity seen in the 600N as opposed to that of the R44; this is attributed to the fact that the 600N has a power-to-weight ratio nearly a third than that of the R44. Wind effects would also have a significant impact on the energy used by the subscale, for it is far more susceptible owing to is lighter weight. A gust that would barely stagger the R44 may push the 600N significantly off course, leading to further energy usage to get back on track. Piloting the subscale with precision proved to be challenging to the pilot, and errors would have been introduced that would increase total fuel usage. Additional factors that could be impacting this include the much higher rotor speed seen by the 600N and vast difference in Froude and Reynolds numbers. The Reynolds number of the 600N is similar in scale to that of many gliders instead of helicopters, and the 600N has a Froude number that is 38.7% that of the R44. Recalling the work done by Chambers, this accounts for a 35.3% difference between the expected and actual ratio. The Froude number, meanwhile, sees a 61.2% difference between the two values, indicating a much more significant impact of gravitational effects as opposed to inertial ones; further reinforcement that weight is the driving parameter when scaling helicopter dimensions previously discussed. This leads to the conclusion that the powerplant used is not a good comparison between the two aircraft. Indeed, the two engines function in different manners and differ in their respective efficiencies. The 600N is intended for short stunt flights rather than transport, so its engine is optimized for power output rather than efficiency; the converse holds true for the R44, which also must consider passenger safety. It is designed for those onboard, rather than simply for stunt flights. Since their intended

uses are very different, combined with the other factors mentined, it is understandable that their energy usage varies so vastly.

Of the real-time modeling and scaling efforts, the author believes that the former will prove to be more useful with regards to urban air mobility applications as opposed to the latter. The main reason for this is the accuracy to which each model successfully completes its task, which has already been discussed. However, another aspect to consider is the powerplant of choice projected to be used by UAM vehicles. Many UAM vehicles are expected to use electric propulsion rather than combustion-based engines, owing to the need for rapid refueling that doesn't expose passengers to unpleasant odors or exhausts greenhouse gases to the environment; one typical example of this is the Joby Aviation UAM prototype[10]. With this in mind, the energy state model is likely of more direct use, as it could be directly implemented to predict energy usage and range of a UAM vehicle, much like is seen in modern automobiles. It could also be used for planning possible destinations the vehicle could reach before requiring refuelling, further saving time.

[10] (Joby Aviation, *Our Story* 2021)

Chapter 6
Conclusions and Future Work

From the scaling methodologies proposed, the Chambers method is most effective when using the helicopter's weight as the primary dimension of interest. The simple scaling laws based on rotor diameter, disk loading, and advance ratio produce excessive errors and are too simplistic to be of use. The model of overall energy use based on the power required for each stage of flight is promising as an estimate of overall and real-time energy usage throughout flight. Further testing is proposed to see if the model will work for predicting real-time energy usage, as the model only draws on commonly available flight data and information from a pilot's handbook rather than fuel usage; this would allow it to be used regardless of powerplant. The model could be used to predict overall range remaining, much akin to those commonly found in automobiles today. The energy scaling methods, however, do not make sense to conclude as effective at this time, as there is significantly greater energy usage in the subscale helicopter than in the full-sized helicopter. This is attributed to their intended uses and other factors mentioned previously.

For future work, which is recommended as there is promise in scaling helicopter performance parameters with an eye towards use with UAM vehicles as well as with helicopters in general, it is proposed to use a more similar powerplant and a specially designed subscale intended to resemble the full-scale helicopter off which it is based. It is also proposed to use scaling methodologies with electric-based rotorcraft, since it is the author's belief that electric UAM vehicles will see use in the near future. For future subscale flight tests, it is proposed that an autonomous system be used for subscale testing if possible, in order to minimize energy losses due to pilot error in staying on course. Finally, for future full-scale flight tests, better coordination with the test pilot is necessary to gathering all data possible during the test flights.

References

[1] Dajani, J. S., Stortstrom, R. G., & Warner, D. B. (1977). (rep.). *The Potential for Helicopter Passenger Service in Major Urban Areas*. Durham, NC: Duke environmental Center.

[2] Raymer, D. P., *Aircraft Design: A Conceptual Approach*, Reston, VA: American Institute of Aeronautics and Astronautics, 2012.

[3] *Robinson R44: Pilot's Operating Handbook*, Torrance, CA: Robinson Helicopter Co., 2007.

[4] Hunt, G. K., "Similarity Requirements for Aeroelastic Models of Helicopter Rotors," *Aeronautical Research Council Current Papers*, Jan. 1972, pp. 3–18.

[5] Chambers, J. R., *Modeling Flight: The Role of Dynamically Scaled Free-Flight Models in Support of NASA's Aerospace Programs*, Washington, D.C.: National Aeronautics and Space Administration, 2010.

[6] "Avgas 100 ll," *Warter Aviation* Available:

https://www.warteraviation.com/fuels/avgas-100-ll/.

[7] Lewis, J., "Morgan Fuels Product Analysis," 2020. Available:

https://morganfuel.com/model-plane-fuel/

[8] LUMITOS. (n.d.). Nitromethane. Retrieved September 20, 2021, from https://www.chemeurope.com/en/encyclopedia/Nitromethane.html.

[9] Elert, G., & Hua, J. (2005). *Energy density of methanol (wood alcohol)*. The Physics Factbook. Retrieved September 28, 2021, from https://hypertextbook.com/facts/2005/JennyHua.shtml.

[10] Joby Aviation. (2021). *Our Story: Joby*. Joby Aviation: Our Story. Retrieved October 24, 2021, from https://www.jobyaviation.com/about/.

Appendix

Table 14: Robinson R44 Raven II Dimensions

Dimension	Value
Length	30 ft
Rotor Diameter	33 ft
Empty Weight	1450 lbs
Maximum Takeoff Weight	2500 lbs
Maximum Disk Loading	2.9230 lb/ft^2
Maximum Airspeed	218.533 ft/sec
Maximum Rotor Rotational Speed	42.726 rad/sec
Maximum Advance Ratio	0.3100
Fuel Tank Capacity	29.5 gal
Fuel Type	100LL Avgas
Fuel Energy Density	112182 BTU/gal
Maximum Power	225 hp
Power/Weight Ratio	0.09 hp/lb
Reynolds Number at Maximum Airspeed	45890175.65
Froude Number at Maximum Airspeed	44.9432

Table 15: Align TREX 600N Dimensions

Dimension	Value
Length	3.806 ft
Rotor Diameter	4.43 ft
Empty Weight	7.05 lbs
Maximum Takeoff Weight	7.81 lbs
Maximum Disk Loading	0.5067 lb/ft^2
Maximum Airspeed	49.85 ft/sec
Maximum Rotor Rotational Speed	188.49 rad/sec
Maximum Advance Ratio	0.0597
Fuel Tank Capacity	0.1162 gal
Fuel Type	30% Nitromethane/47% Methanol Mixture
Fuel Energy Density	40946 BTU/gal
Maximum Power	2.1 hp @ 17000 rpm
Power/Weight Ratio	0.2689 hp/lb
Reynolds Number at Maximum Airspeed	1405263.096
Froude Number at Maximum Airspeed	17.4209